CrossMark

Microstructure and magnetic properties of Nd–Fe–B sintered magnets with P addition

Fang Yang, Guang-Le Dong, Yan-Li Sui, Si-Yang Ye, Ping Li, Cun-Guang Chen, Xue-Xu Gao, Zhi-Meng Guo*

Abstract In this paper, the effects of P doping on magnetic properties and microstructure were studied in Nd–Fe–B sintered magnets. With P doping, the grain size gets refined and the distribution of the main phase is optimized due to the reduction of the liquidus temperature. The liquidus temperature for the 0.05 wt% P-doped magnets is 1022 K, while that for the P-free magnets is 1038 K. As P content increases, the liquidus temperature significantly decreases. Clear and continuous grain boundary phases are formed in the P-containing magnets with smaller grain size. The optimized microstructure with average grain size of 8.43 μm is obtained in the 0.05 wt% P-doped magnets, which is approximately 0.69 μm smaller than that of P-free sintered magnets (9.12 μm). Though P is usually thought to be an impurity element, it might be beneficial in Nd–Fe–B sintered magnets with proper addition. The coercivity of the 0.05 wt% P-doped magnets could be increased to 1283 kA·m^{-1}, with slight changes of the remanence and the maximum magnetic energy product. NdPO$_4$ phases in the grain boundary are of hexagonal structure, while those at the triple junctions have monoclinic structure. Activated sintering is achieved by doping proper P element in the Nd–Fe–B sintered magnets.

F. Yang, P. Li, C.-G. Chen, Z.-M. Guo*
Institute of Advanced Materials and Technology, University of Science and Technology Beijing, Beijing 100083, China
e-mail: zmguo@ustb.edu.cn

G.-L. Dong
Tianjian Sanhuan Lucky New Materials Inc., Tianjin 300457, China

Y.-L. Sui, S.-Y. Ye, X.-X. Gao
State Key Laboratory for Advanced Metals and Materials, University of Science and Technology Beijing, Beijing 100083, China

1 Introduction

In the last two decades, there has been a rapid growth in the permanent magnet electric motors and generators of (hybrid) vehicles industries [1, 2]. Nd–Fe–B sintered magnets have gained considerable attention due to their excellent magnetic properties of high maximum energy product and coercivity [3–5]. Typical Dy-free sintered Nd–Fe–B magnets with a coercive field ($\mu_0 H_c$) of ∼ 1.5 MA·m^{-1} are sufficient for most room temperature applications [6, 7]. However, low Curie temperature and thermal stability limit their applications at high temperature above 473 K. At elevated temperatures, the effects of thermal activation on the reversal process increase, resulting in a significant reduction in coercivity [8–10]. Heavy rare earth elements such as Dy are commonly added to increase the coercivity in Nd–Fe–B sintered magnets. Partial substitution of Dy for Nd in the 2:14:1 phase is known to form a (Nd, Dy)$_2$Fe$_{14}$B shell with higher magnetic anisotropy field at the outer region of the main phase grains [5, 11–14]. However, there is a strong demand to achieve high coercivity without using Dy due to its scarcity and high cost.

It is well known that the magnetic properties can be improved by controlling the microstructure, especially addition of non-rare earth elements [15–17]. Numerous efforts have revealed that inhibiting grain growth, retaining grain boundaries and lowering melting point of Nd-rich phases are effective to increase the coercivity. Some researchers have reported that the addition of small amounts of Mo, W and Nb to Nd–Fe–B sintered magnets is

effective in inhibiting grain growth [18–21]. The grain boundaries of Nd–Fe–B sintered magnets were improved with addition of small amounts of Al, Ga or Cu [22–24]. On the other hand, it was reported that the fine-grained Nd–Fe–B sintered magnets exhibit large coercivity (H_c) of 1.85 T by the addition of low-C concentrations [25]. As we know, P is thought to be a harmful element in most aspects of materials. Recently, Zhang et al. [26] found that a coercivity enhancement was obtained after the addition of P to Fe–Pt–B alloys. With P addition, the liquidus temperature of the alloy was lowered [27, 28]. However, little is known about the effect of P addition on the microstructure and magnetic properties of Nd–Fe–B sintered magnets. The research about P introduction in the magnets was rarely reported.

In this study, the effect of small amount of P on microstructure and magnetic properties of Nd–Fe–B magnets was investigated. In addition, the mechanism of grain refinement with P introduction in the magnets was established. The magnetic and microstructural properties of P-doped magnets were compared with those of P-free magnets.

2 Experimental

2.1 Materials preparation

The commercial Nd–Fe–B and P powders were used as the raw materials. The purity of the raw materials was over 99%. Nd–Fe–B powders ($\sim$ 5 μm) with a nominal composition of 31.0Re(Re–Nd, Pr)–0.5Dy–bal.Fe–1.0B–4.0 M (wt%, M–Cu, Al, Co, Cr, Ga) were mixed with various amounts of commercially available P (0 wt%, 0.05 wt%, 0.10 wt%, 0.20 wt%) powders. This was performed by ball milling for 2 h using SPEX-8000 mixer/mill with a steel ball-to-powder weight ratio of 5:1. The average particle size of P powder was about 5 μm. After being pressed in a magnetic field of 1352 kA·m^{-1}, the green compacts were vacuum-sintered at 1323 K for 3 h. Subsequently, the magnets were annealed at 1203 K for 3 h following subsequent annealing at 758 K for 6 h.

2.2 Microstructural and properties characterization

The magnets were cut into cylinder shape with a dimensional size of Φ 8 mm × 5 mm by wire electrode cutting. Four samples of each P content were conducted to confirm reproducibility. Densities of the sintered magnets were determined by Archimedes' principle measurement. The room temperature magnetic properties of the processed magnets by mechanical polishing were measured by a magnetic measurement device NIM-200C (National Institute of Metrology, PR China). The characterization of the samples by differential scanning calorimetry (DSC, NETZSCHSTA449) was performed using 200-mg crushed sintered magnets in an alumina box under protective Ar gas. Microstructural studies were conducted by backscattered scanning electron microscope (SEM, Supra55) equipped with an energy-dispersive spectroscopy detector (EDS), using monochromatic Cu Kα radiation with the wavelength of X-ray 0.154 nm and operated at 40 kV as well as 150 mA. Elemental distribution was performed using electron probe microanalysis (EPMA, JEOL, JXA-8230) operated at 0.2–30.0 kV as well as 1×10^{-12}–1×10^{-5} A. Phase composition and identification were operated by transmission electron microscope (TEM, JEM2010) combined with energy-dispersive spectroscopy detector (EDS) and selected area electron diffraction (SAED). Thin foil specimens for TEM analysis were prepared using an ion milling system.

3 Results and discussion

3.1 Magnetic properties

All sintered Nd–Fe–B magnets were crack-free. The densities of the magnets are above 7.5 g·cm^{-3}, as shown in Table 1. With the increase in P content, the density of the Nd–Fe–B sintered magnets decreases. The density for the 0.20 wt% P-doped magnets decreases from 7.59 to 7.52 g·cm^{-3}.

Table 1 also shows the magnetic properties of the P-containing magnets as a function of P content. The measured coercivity (H_c), remanence (B_r) and maximum magnetic energy product ((BH)$_{max}$) of the undoped magnets are 1236 kA·m^{-1}, 1.230 T and 292.2 kJ·m^{-3}, respectively. Compared with the undoped magnets, the coercivity for the 0.05 wt% P-doped magnet increases from 1236 to 1283 kA·m^{-1} and the peak value is 3.8% higher than that of P-free magnets. In addition, there is no noticeable changes in B_r and (BH)$_{max}$. Proper P addition is beneficial to improve the coercivity in Nd–Fe–B sintered magnets. Upon further increasing P content, the magnetic

Table 1 Magnetic properties of P-doped Nd–Fe–B magnets as functions of P content

P content/ wt%	Density/ (g·cm^{-3})	H_c/ (kA·m^{-1})	B_r/T	(BH)$_{max}$/ (kJ·cm^{-3})	H_k/ H_{cj}
0	7.59 ± 0.01	1236	1.230	292.2	0.97
0.05	7.57 ± 0.01	1283	1.227	290.9	0.96
0.10	7.56 ± 0.01	1254	1.222	288.3	0.96
0.20	7.52 ± 0.01	1206	1.219	287.5	0.95
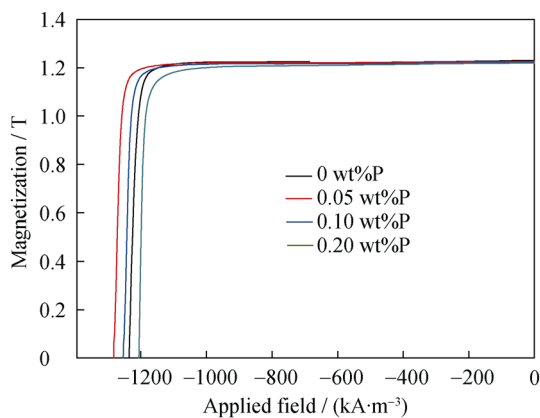
Fig. 1 Demagnetization curves for P-doped Nd–Fe–B sintered magnets

Fig. 2 DSC curves of Nd–Fe–B sintered magnets with P addition (x = 0 wt%–0.20 wt%)

properties significantly decrease. With 0.10 wt% P addition, the coercivity decreases from 1283 to 1254 kA·m^{-1}. The introduction of 0.20 wt% P results in obvious decrease in coercivity and remanence. The coercivity decreases to 1206 kA·m^{-1}, and the peak value is 6.0% lower than that of 0.05 wt% P-doped magnet, as shown in Table 1. And the corresponding B_r decreases from 1.227 to 1.219 T. Also, $(BH)_{max}$ decreases from 290.9 to 287.5 kJ·m^{-3}. Figure 1 compares corresponding demagnetization curves of P-free and P-doped magnets. It is obvious that the coercivity gets enhanced when P content is not more than 0.10 wt%. Excessive P introduction leads to a deterioration in density and magnetic performance.

The introduction of P in P-doped magnets may cause the changes of grain size distribution or change the structure of grain boundaries. To understand the effects of P doping on microstructure and magnetic performance in magnets, DSC, FESEM, EPMA and TEM investigations were conducted.

3.2 DSC curves

Figure 2 shows DSC curves of Nd–Fe–B sintered magnets as a function of P content. DSC analysis was performed from room temperature to 1323 K at a constant heating rate of 0.67 K·s^{-1}. Two endothermic peaks are observed on all DSC curves. The first temperature, T_{x1}, corresponds to Curie temperature of Nd$_2$Fe$_{14}$B phase, while the second endothermic peak, T_{x2}, corresponds to the melting point of Nd-rich eutectic phases. Compared with P-free magnets, T_{x1} remains about the same in P-containing magnets. And the first temperature T_{x1} is close to 600 K. In the undoped magnets, the second temperature, T_{x2}, is 1038 K. When P content is 0.05 wt%, temperature decreases to 1022 K. The second temperature decreases to 1013 K with 0.20 wt% P, as shown in Fig. 2. The second temperature decreases with P content increasing. During sintering, Nd-rich eutectic
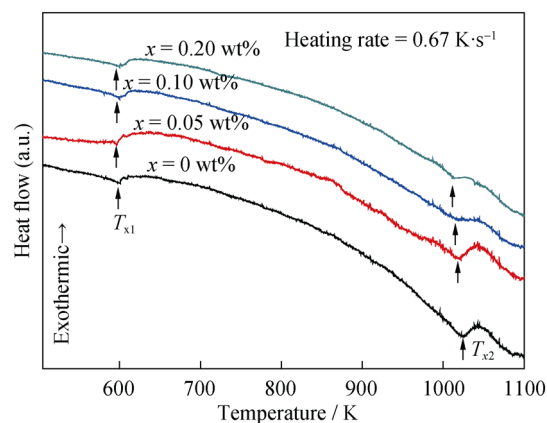
phases precipitate in a liquid form at T_{x2}. It suggests that the liquidus temperature is lowered with P addition. P doping reduces the melting point and increases the fluidity of the liquid Nd-rich phase during sintering.

3.3 Microstructures

Figure 3 shows the microstructure changes and grain size distribution in the magnets with different P contents. Figure 3a shows typical microstructure of the sintered magnets, in which the dark gray corresponds to Nd$_2$Fe$_{14}$B matrix phase and the bright regions are various Nd-rich intergranular phases. The Nd-rich grain boundary phases (GBPs) are unclear and discontinuous between two ferromagnetic Nd$_2$Fe$_{14}$B phase grains. Besides, the 2:14:1 phase grains are not uniform and the grain size is relatively large. With P doping, distributions of GBPs and the main phase grain size are optimized, as shown in Fig. 3b. Compared with P-free magnets, clear and continuous GBPs are formed in P-doped magnets, which is beneficial to diminish the magnetic exchange interactions between neighboring grains and enhance the magnetic isolations.

In P-free magnets, the average grain size is 9.12 μm. The grain size is relatively small, and the grain size distribution is more uniform in P-doped magnets, as shown in Fig. 3e, f. The average grain size of 0.05 wt% P-doped magnets decreases to 8.43 μm, which is approximately 0.69 μm less than that of P-free magnets. When P content increases to 0.20 wt%, the average grain size reduces to 7.88 μm. But there exist obvious defects, as shown in Fig. 3c, which may work against the magnetic performance. It can be indicated that the grain growth gets inhibited with P addition. Additionally, Nd$_2$Fe$_{14}$B phase grains become rounder and more uniform, indicating that the wettability between the main phase and the intergranular phase gets improved. As a result, in the 0.05 wt%
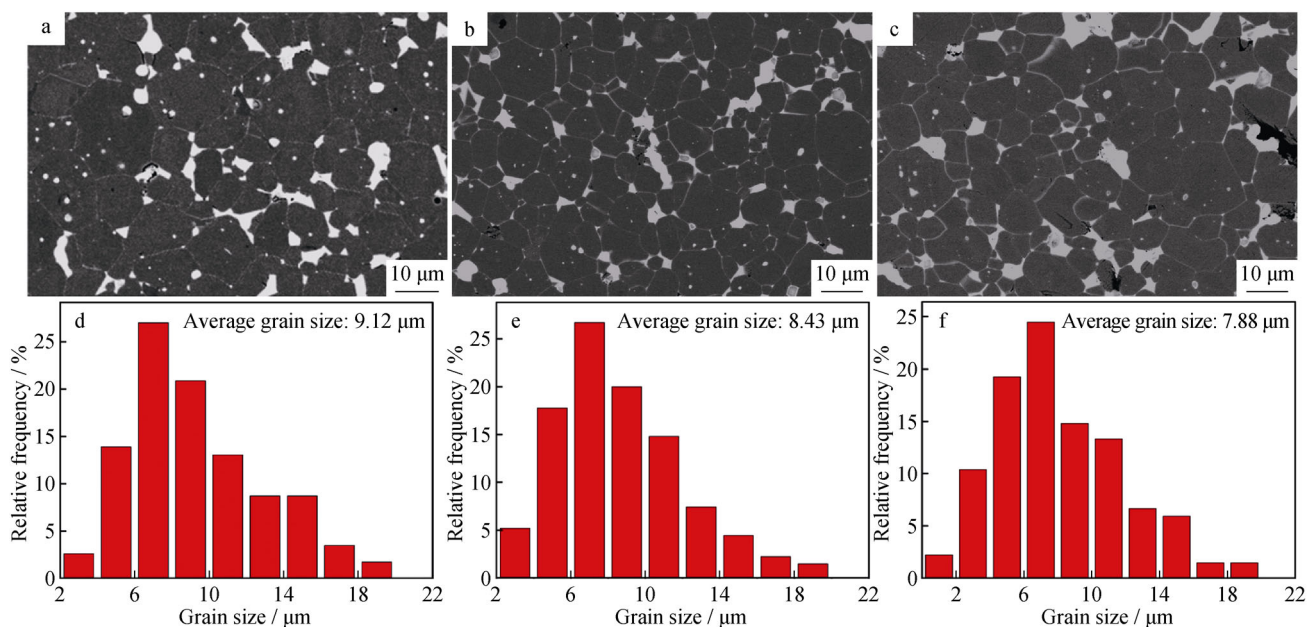
Fig. 3 SEM images and grain size distribution of magnets with different P contents: **a**, **d** 0 wt%; **b**, **e** 0.05 wt%; **c**, **f** 0.20 wt%

P-doped magnets, the coercivity gets enhanced with the remanence slightly changing. Excessive P introduction leads to the deterioration of the magnetic properties. Probably, the reduction of the magnetic properties occurs due to the decrease in the density and the content of the main phase. It can be inferred that proper P introduction promotes the uniformity and continuity of GBPs because the melting point decreases during sintering [29].

3.4 Phase distribution and composition

Figure 4 shows the distribution of Nd, O and P in the undoped and 0.05 wt% P-doped magnets. It can be observed that Nd is dominant in the intergranular phases

and O is also enriched in the phases. Both Nd and O are the essential components of Nd-rich phase at the triple junctions. NdO_x oxides are the main form of Nd-rich phases. The distribution of P in the P-containing magnets is not uniform. P is enriched in Nd-rich phases, just like the white mark shown in Fig. 4b. It can be inferred that P-containing precipitates may be phosphorus oxide phases.

To further characterize elemental distribution, the spatial distribution of Fe, P, Nd and O across the main phase and intergranular phase was measured by EDS line-scan. Figure 5b–e shows the composition variation across the region. P is clearly enriched in Nd-rich phases. The distribution of P is not uniform, and obvious clustering is observed. There are no P-precipitates in the main phases. In
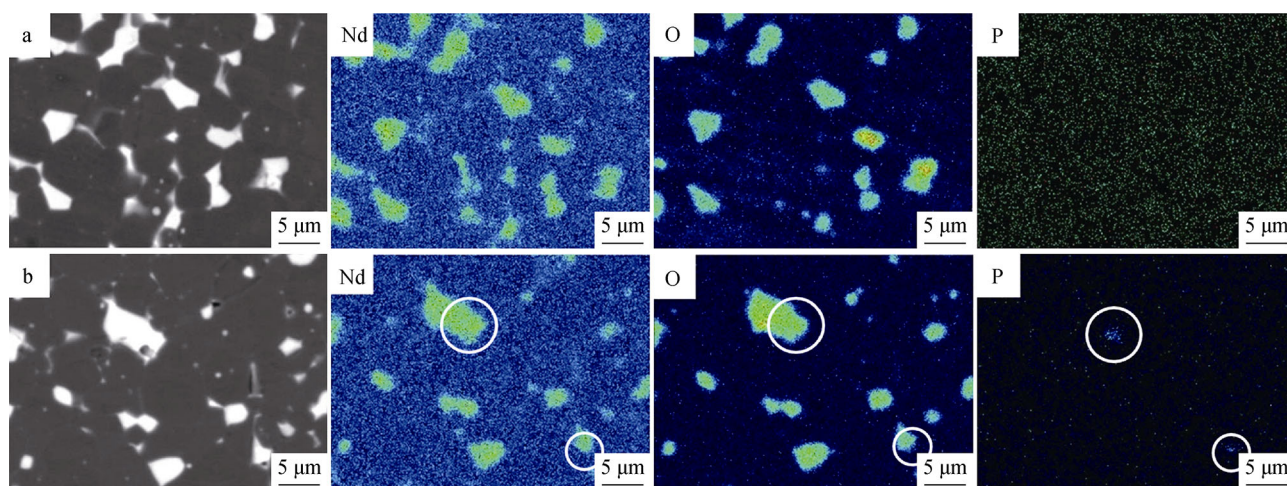
Fig. 4 SEM images and EPMA mapping images of Nd, O and P elements of magnets with different P contents: **a** 0 wt% and **b** 0.05 wt%
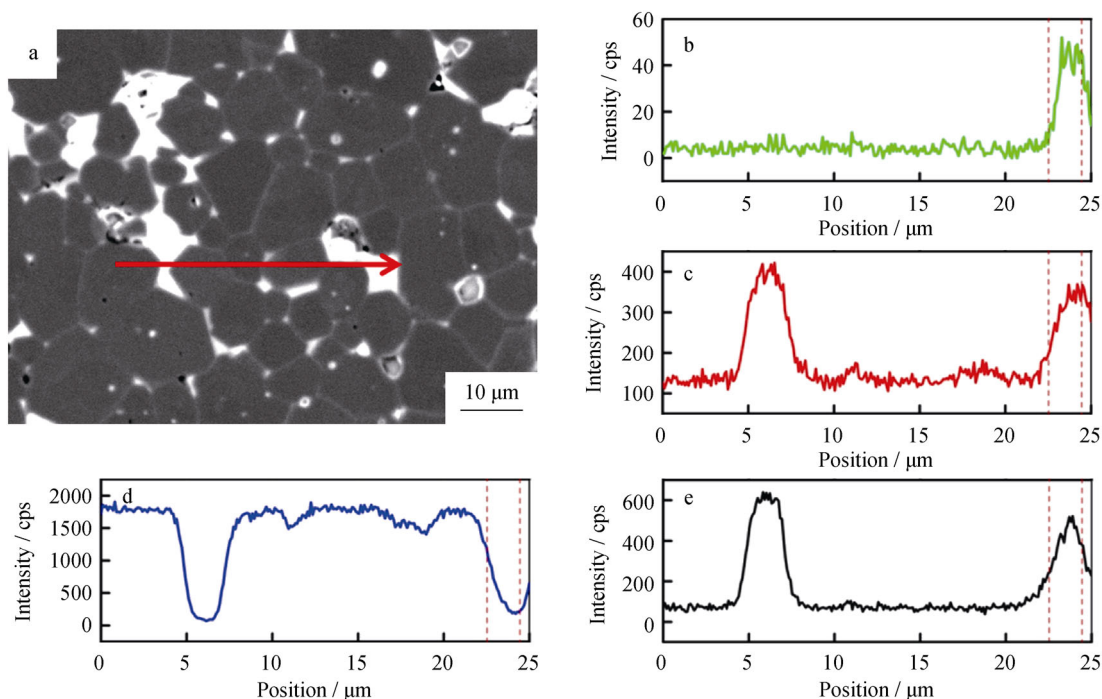
Fig. 5 High-magnification backscattered SEM images and EDS patterns in 0.05 wt% P-doped magnets: **a** SEM images and line-scan profiles for **b** P, **c** Nd, **d** Fe and **e** O indexed as red arrow in **a**
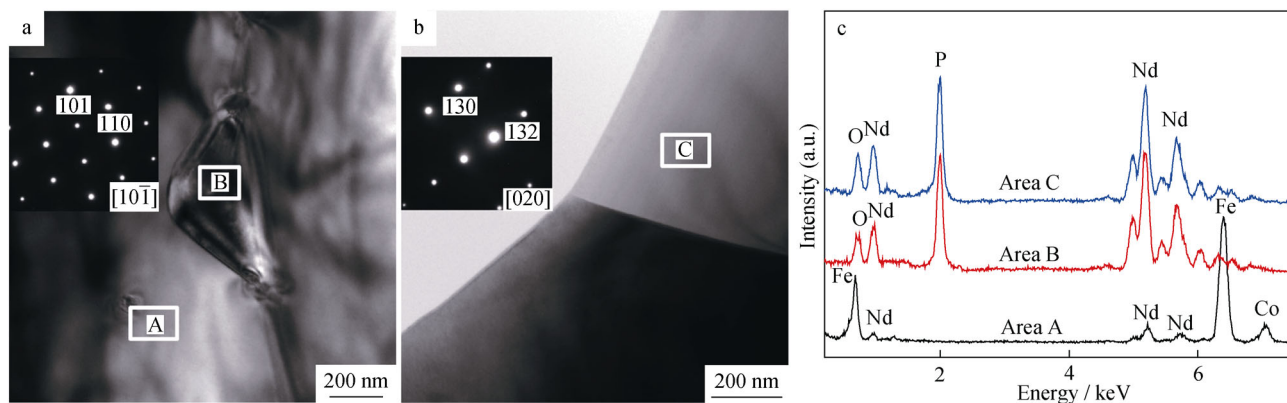
Fig. 6 TEM images and SAED patterns of **a** $NdPO_4$ phase in GBPs, **b** $NdPO_4$ phase at triple junctions, and **c** EDS results of areas A–C in 0.05 wt% P-doped magnets

P-rich phases, there exist Nd, O and P. It can be inferred that the potential form of P-rich phase might be NdO_xP_y phase.

Figure 6 presents TEM images and EDS results of the phosphorus oxide phases in 0.05 wt% P-doped magnets. Particularly interesting is the observation that P-rich phase is found to simultaneously exist in the grain boundary and in the triple junctions. Corresponding SAED patterns show that P-precipitates are $NdPO_4$ phases. $NdPO_4$ phase in the grain boundary is identified as hexagonal structure with lattice parameters of $a = 0.698$ nm, $b = 0.698$ nm and $c = 0.634$ nm, as shown in Fig. 6a. But, the grain size of

$NdPO_4$ phase is large. In addition, SAED patterns of $NdPO_4$ phase at the triple junctions are matching to the monoclinic structure, with lattice parameters of $a = 0.674$ nm, $b = 0.696$ nm and $c = 0.641$ nm. EDS results also confirm that $NdPO_4$ phase tends to precipitate in different regions.

4 Conclusion

In summary, the effects of P doing on magnetic properties and microstructure in Nd–Fe–B sintered magnets were

investigated. The melting point of Nd-rich eutectic phase is lowered with P content increasing, leading to the wettability improvement and grain growth inhibition. In 0.05 wt% P-doped magnets, the melting point decreases from 1038 to 1022 K. And, the average grain size and grain size distribution are optimized, with forming clear and continuous GBPs. As a result, the magnets with 0.05 wt% P addition show a larger coercivity of 1283 kA·m^{-1}, without notable changes in remanence and the maximum magnetic energy product, as compared to that of the undoped magnets. In the P-containing magnets, NdPO$_4$ phases mainly are precipitated in the grain boundary and triple junctions. Though P acts as a harmful element in most aspects of materials, it is beneficial for activating sintering with proper addition in Nd–Fe–B sintered magnets.

References

[1] Krishna SC, Jha AK, Pant B, George KM. Microstructure and magnetic properties of hot-deformed anisotropic Nd–Fe–B magnets prepared from amorphous precursors with different crystallization proportions. Rare Met. 2017;35(4):263.

[2] Ma Q, Zhu JT, Zhang XF, Zhao ZR, Liu YL, Wang GF, Li YF, Li ZB. Achievement of high performance of sintered R–Fe–B magnets based on misch metal doped with PrNd nanoparticles. Rare Met. 2018;37(3):1.

[3] Cui XG, Wang XH, Cui CY, Yin GC, Xia CD, Fang C. Research progress in grain boundary diffusion modification, microstructures and propertis of sintered Nd–Fe–B magnets. Chin J Rare Met. 2018;42(3):315.

[4] Bance S, Fischbacher J, Schrefl T. Thermally activated coercivity in core–shell permanent magnets. J Appl Phys. 2015;117(17):821.

[5] Liu WQ, Chang C, Yue M, Yang JS, Zhang DT, Zhang JX, Liu YQ. Coercivity, microstructure, and thermal stability of sintered Nd–Fe–B magnets by grain boundary diffusion with TbH$_3$ nanoparticles. Rare Met. 2017;36(9):718.

[6] Yang MN, Wang H, Hu YF, Yang LYM, Maclennan A, Yang B. Relating atomic local structures and curie temperature of NdFeB permanent magnets: an X-ray absorption spectroscopic study. Rare Met. 2017. https://doi.org/10.1007/s12598-017-0918-5.

[7] Wang Z, Liu WQ, Zhang DT, Yue M, Huang XL, Li XL. Enhancement of corrosion resistance in sintered Nd–Fe–B permanent magnet doping with different CuZn$_5$ contents. Rare Met. 2017;36(10):812.

[8] He JZ, Lin T, Shao HP, Zhao LW, Zhao DC. 3D printing of NdFeB rare earth permanent magnet. Chin J Rare Met. 2018;42(6):657.

[9] Loewe K, Brombacher C, Katter M, Gutfleisch O. Temperature-dependent Dy diffusion processes in Nd–Fe–B permanent magnets. Acta Mater. 2015;83:248.

[10] Shi XN, Zhu MG, Han R, Song LW, Li W. Corrosion behavior of dual-main-phased (Nd$_{0.8}$Ce$_{0.2}$)$_2$Fe$_{14}$B magnets with and without annealing process. Rare Met. 2017. https://doi.org/10.1007/s12598-017-0963-0.

[11] Wei HD, Qian Y, Qian H, Zhang B, Xiang BJ, Jia XF. Effect of grain edge region modification on the coercivity of sintered NdFeB magnets. Chin Rare Earth. 2017;38(3):56.

[12] Doser M, Keeler G. Long-term stability of Fe–B–Nd–Dy alloys made by Dy$_2$O$_3$ additions. J Appl Phys. 1988;64(10):5311.

[13] Li WF, Sepehri-Amin H, Ohkubo T, Hase N, Hono K. Distribution of Dy in high-coercivity (Nd, Dy)–Fe–B sintered magnet. Acta Mater. 2011;59(8):3061.

[14] Park SE, Kim TH, Lee SR, Kim DH, Nam-Kung S, Jang TS. Magnetic and microstructural characteristics of Nd–Fe–B sintered magnets doped with Dy$_2$O$_3$ and DyF$_3$ powders. IEEE Trans Magn. 2011;47(10):3259.

[15] Li WF, Ohkubo T, Hono K. Effect of post-sinter annealing on the coercivity and microstructure of Nd–Fe–B permanent magnets. Acta Mater. 2009;57(5):1337.

[16] Mo WJ, Zhang LT, Liu QZ, Shan AD, Wu JS, Komuro M. Dependence of the crystal structure of the Nd-rich phase on oxygen content in an Nd–Fe–B sintered magnet. Scr Mater. 2008;59(2):179.

[17] Kim TH, Lee SR, Namkumg S, Jange TS. A study on the Nd-rich phase evolution in the Nd–Fe–B sintered magnet and its mechanism during post-sintering annealing. J Alloys Compd. 2012;537(19):261.

[18] Jin WK, Lee WS, Byun JM, Kim SH, Kim YD. Grain refinement in heavy rare earth element-free sintered Nd–Fe–B magnets by addition of a small amount of molybdenum. J Appl Phys. 2015;117(17):17B523.

[19] Chu TY, Chin TS, Lin CH, Yao JM. Evidence of domain-wall pinning in W-doped (NdDy)(FeCo)B sintered magnets. J Appl Phys. 1994;76(10):6834.

[20] Cheng WH, Li W, Li CJ, Li XM. The role of Nb addition in Nd–Fe–B sintered magnets with high performance. J Alloys Compd. 2001;319(1):280.

[21] Shen X, Wang Y, Diao Z, Liu X. The effect of molybdenum on the magnetic properties of the Nd–Fe–Co–B system. J Appl Phys. 1987;61(8):3433.

[22] Hu SQ, Peng K, Chen H. Influence of annealing temperature on the Dy diffusion process in NdFeB magnets. J Magn Magn Mater. 2017;426:340.

[23] Fidler J, Bernardi J, Schrefl T. Permanent magnets—new microstructural aspects. Scr Mater. 1995;33(10–11):1781.

[24] Pandian S, Chandrasekaran V, Markandeyulu G, Iyer KJL, Rama-Rao KVS. Effect of Al, Cu, Ga, and Nb additions on the magnetic properties and microstructural features of sintered NdFeB. J Appl Phys. 2002;92(10):6082.

[25] Sasaki TT, Ohkubo T, Une Y, Kubo H, Sawawa M, Hono K. Effect of carbon on the coercivity and microstructure in fine-grained Nd–Fe–B sintered magnet. Acta Mater. 2015;84:506.

[26] Zhang W, Kazahari A, Yubuta K, Makino A, Wang YM, Umetsu R. Effect of P addition on the structure and magnetic properties of melt-spun Fe–Pt–B alloy. J Alloys Compd. 2014;586(4):S294.

[27] Massalski TB. Binary Alloy Phase Diagrams. Ohio: ASM International; 1990. 28.

[28] Huang PY. Powder Metallurgy. Beijing: Metallurgical Industry Press; 1997. 296.

[29] Bae KH, Lee SR, Kim HJ, Lee MW, Jang TS. Effect of WS$_2$/Al co-doping on microstructural and magnetic properties of Nd–Fe–B sintered magnets. J Alloys Compd. 2016;673:321.